COBEM2015

ABCM Associação Brasileira de Engenharia e Ciências Mecânicas

23rd ABCM International Congress of Mechanical Engineering
December 6-11, 2015, Rio de Janeiro, RJ, Brazil

COMPUTER SIMULATION OF HYDRAULIC FRACTURING USING FINITE ELEMENTS WITH HIGH ASPECT RATIO

Pedro Rogério Cleto[1]
pedro.constant@gmail.com
Osvaldo Luís Manzoli[1]
omanzoli@feb.unesp.br
Michael Andrade Maedo[1]
michaelmaedo@yahoo.com.br
Leonardo José do Nascimento Guimarães[2]
leonardo@ufpe.com

[1]São Paulo State University - UNESP - Bauru/SP - Av. Eng. Luiz Edmundo Coube, 14-01, CEP: 17033-360
[2]Federal University of Pernambuco - UFPE - Recife/PE - Av. Prof. Moraes Rego, 1235, CEP: 50670-901

Abstract. *The extraction and production of shale gas has gained importance in the oil industry over the past few years due to its economic viability. However, the shale permeability is low, a fact that complicates the extraction of gas. Hydraulic fracturing is a technique that is able to increase the permeability of the shale by injecting fluid at high pressure into the well. This work contributes to the generation of numerical tools to study the formation and propagation of the fractures generated hydraulically, considering an explicit type of hydro-mechanical coupling. Fractures are modeled through the Mesh Fragmentation Technique (MFT), which consists of inserting nonlinear solid finite elements with a high aspect ratio between the bulk elements of the mesh. The behavior of the fluid is described by Darcy's Law. Some numerical analyses of leak-off tests in 2D wells are carried out considering different boundary conditions and types of meshes. The results show that the MFT is able to reproduce the fracturing process in accordance with experimental results, presenting a pressure drop due to the hydraulic fracturing process. As expected, the fractures propagate perpendicular to the smallest principal stress in all cases. Since the fractures must follow the interface elements, surrounding the standard (bulk) elements, the use of unstructured meshes is recommended to avoid mesh dependence.*

Keywords: *hydraulic fracturing, hydro-mechanical coupling, mesh fragmentation*

1. INTRODUCTION

The hydraulic fracturing process came to prominence a few years ago in the global context, influenced mainly by the wide application in American deposits of shale gas. Performing hydraulic fracturing tests is relatively expensive and has limitations, especially in relation to the scale. Thus, the numerical simulations are a very viable alternative for the study of this process, allowing play scenarios that would be impossible to be made in the laboratory. Hydraulically fracturing a medium consists of continuously injecting a particular fluid under high pressure at an internal point of this medium. Over time, the fluid pressure tends to increase until the moment that the medium can no longer resist and then fractures.

The Finite Element Method is one of the most renowned computational techniques in engineering, having numerous applications, including hydraulic fracturing studies. However, the characterization of discontinuities, i.e., fractures, remains a challenge to the academic community. Since the hydraulic fracturing is a multiphysical problem a coupled solutions are required.

Rouainia *et al.* (2006) used two tools to analyze the hydraulic fracturing process through a coupling relation. The first tool consists of using the finite element method to understand the hydraulic behavior of the system, considering that this obeys the Darcy's Law. The second tool consists of using the Discontinuous of Strain Analysis Method for analyzing the discontinuous deformable solid phase. The authors were able to show the opening and closing of pre-existing fractures in the medium.

Li *et al.* (2012), by means of the Finite Element Method, proposed a three-dimensional model that considers the coupling between three processes: mechanical deformation of the solid medium induced by fluid pressure acting on the surface of the fracture; the flow of fluid within the fracture; and the propagation of the fracture. They were able to show that the propagation of the fracture occurs in the direction of maximum principal stress.

This paper proposes the use of mesh fragmentation technique, which consists of inserting solid finite element with a high aspect ratio (interface elements) in between adjacent elements of the original mesh (Manzoli *et al.*, 2012; Maedo *et al.*, 2014), which in turn have a formulation based on Continuous Strong Discontinuity Approach (CSDA) (Oliver *et al.*, 1999; Oliver, 2000; Oliver and Huespe, 2004), to model the onset and propagation of the fracture. Mechanical and hydraulic properties are attributed to elements of high aspect ratio, so that, by means of the parallel plates law, the discontinuity caused by the fracture and the flow of fluid can be coupled. The fragmentation technique analysis can be fully carried out in the context of continuum mechanics, facilitating interpretation and eliminating the use of specific algorithms to track crack paths.

2. SOLID FINITE ELEMENT WITH HIGH ASPECT RATIO

Let us consider a linear triangular element, with base b defined by the distance between nodes 1 and 3 and height h defined by the distance between nodes 1 and 2, as shown in Fig. 1.

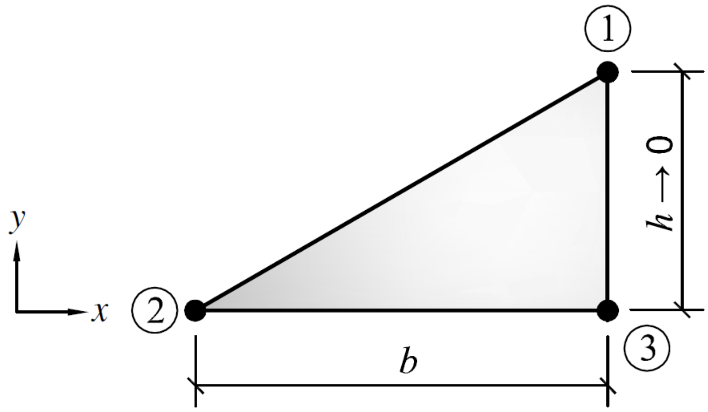

Figure 1. Interface solid finite element.

Thus, it is defined that the hydraulic gradient is given by:

$$\boldsymbol{\nabla} P = \begin{bmatrix} 0 & -\frac{1}{b} & \frac{1}{b} \\ \frac{1}{h} & 0 & -\frac{1}{h} \end{bmatrix} \begin{bmatrix} P_1 \\ P_2 \\ P_3 \end{bmatrix} = \begin{bmatrix} \frac{1}{b}(P_3 - P_2) \\ \frac{1}{h}[\![P]\!] \end{bmatrix} \tag{1}$$

where P_1, P_2 and P_3 are the pressures in nodes 1, 2 and 3, respectively, and $[\![P]\!]$ is the pressure jump, given by:

$$[\![P]\!] = P_1 - P_3 \tag{2}$$

The fluid flow in the element can finally be written as:

$$\boldsymbol{q} = -\frac{(k\boldsymbol{I})}{\mu}\boldsymbol{\nabla} P \tag{3}$$

where μ is the viscosity of the fluid, k is the intrinsic permeability of the element and $\boldsymbol{I}$ is the second order unit tensor.

3. HYDROMECHANICAL COUPLING

When two or more physical systems interact influence one another whose relation happens to varying degrees of interaction, one can consider it a coupled problem. In the case of a reservoir, the relation between stress and flux (among other things) characterizes a coupled problem, considering that, computationally, the stress and fluid analysis code comprise a single structure (Yaquetto, 2011).

For this work we use the explicit coupling method. In this case the communication between mechanical and flow models is weak because changes in pressure field causes deformation in the rock mass, but variations in the stress state does not affect the pressure in the pores. In gas reservoirs the explicit coupling may be used without significant problems because the gas compressibility overlaps to the rock compressibility (Yaquetto, 2011; Naveira, 2008).

3.1 Parallel Plates Model

The parallel plates model (Huitt, 1956; Snow, 1965) was used to relate the hydraulic conductivity of a fracture with its aperture. Therefore, let us consider that the walls of the fracture can be represented by two smooth parallel plates, both plane surface, separated by an aperture. Thus, the permeability of the fracture can be written is terms of its aperture (Witherspoon *et al.*, 1980; Marin, 2011), i.e.:

$$k_f = \frac{w^2}{12} \tag{4}$$

where k_f is the permeability of the fracture and w is its aperture, given by separation distance between the plates.

4. BALANCE EQUATIONS

The adopted hydromechanical model allows to relate more realistically mechanical and hydraulic physical phenomena in a coupled way. Therefore, it is considered that changes in the fluid pressure field influence the rock stress field. Consequently, when the rock exceed its tensile strength, the discontinuity created will have a permeability much higher than the rock. Therefore, the pressures field will undergo significant changes, which will impact directly on the stresses, thus constituting a closed loop.

First, to the mechanical problem, it was considered the stress balance equation given by:

$$\boldsymbol{\nabla} \cdot \boldsymbol{\sigma} + \boldsymbol{b} = 0 \tag{5}$$

where $\boldsymbol{\sigma}$ is the total stress tensor and $\boldsymbol{b}$ is the body force vector.

According to the Terzaghi's Effective Stress Principle, the total stress is related to the effective stress as follows:

$$\boldsymbol{\sigma} = \bar{\boldsymbol{\sigma}} + P\boldsymbol{I} \tag{6}$$

where $\bar{\boldsymbol{\sigma}}$ is the effective stress tensor, P is the fluid pressure exerts on the solid and $\boldsymbol{I}$ is the second order unit tensor. The effective stresses are responsible for the variations of motion, i.e., displacements and deformations. The effective stress tensor, in turn, can be written as follows:

$$\bar{\boldsymbol{\sigma}} = \Sigma(\boldsymbol{\epsilon}) \tag{7}$$

where the effective stress is written in terms of the strain tensor, $\boldsymbol{\epsilon}$, by means of a constitutive relation Σ.

The strain tensor $\boldsymbol{\epsilon}$ can be divided into two parts, volumetric and deviatoric, i.e.:

$$\boldsymbol{\epsilon} = \boldsymbol{\epsilon_v} + \boldsymbol{\epsilon_d} \tag{8}$$

where $\boldsymbol{\epsilon_v}$ is the volumetric part and $\boldsymbol{\epsilon_d}$ is the deviatoric part. Manzoli *et al.* (2012) and Maedo *et al.* (2014) show how $\boldsymbol{\epsilon_v}$ and $\boldsymbol{\epsilon_d}$ of the interface solid finite element are relate to h and b.

For the hydraulic problem, it is considered that the fluid flow may be governed by mass balance equation of the liquid phase, which is given by:

$$\frac{\partial \phi S \rho}{\partial t} + \boldsymbol{\nabla} \cdot (\rho_0 \boldsymbol{q}) + Q = 0 \tag{9}$$

The first term Eq. (9) is called storage term, which varies with time t, where ϕ is the rock's porosity, S is the rock's degree of saturation (which was considered fully saturated, then S=1) and ρ is the density of the liquid, which is a function of pressure. Thus, it was considered an exponential law of variation of the density of the liquid relative to the pressure variation in it, given by:

$$\rho = \rho_0 e^{\beta(P-P_0)} \tag{10}$$

where ρ_0, which also appears in the second term of Eq. (9), is the reference density of the fluid for a given reference pressure P_0 and β is the fluid's isothermal compressibility factor.

The second term of the Eq. (9) refers to the behavior of the liquid phase, where $\boldsymbol{q}$ is the flux vector, given by Darcy's Law. This law allows to describe the laminar flux of Newtonian fluids in porous media. Therefore, the flow of fluid with respect to solid phase is given by:

$$\boldsymbol{q} = -\frac{(k\boldsymbol{I})}{\mu} \boldsymbol{\nabla} P \tag{11}$$

where μ is the fluid's viscosity, k is the intrinsic permeability of the porous media, $\boldsymbol{I}$ is the second order unit tensor and P corresponds to the fluid pressure.

The third term, Q, is the source or sinkhole of fluid.

5. CONTINUOUS DAMAGE MODEL

The damage model adopted for expressing the degradation suffered by the rock is expressed by the following equation:

$$\bar{\boldsymbol{\sigma}} = \Sigma(\boldsymbol{\epsilon}) = (1-d)\boldsymbol{C} : \boldsymbol{\epsilon} \tag{12}$$

where $\boldsymbol{C}$ is the fourth order elastic constitutive tensor and d is the damage scalar variable, which can range from 0 (intact material) to 1 (fully degraded material).

5.1 Tensile damage model

The damage criterion is based on the component of the stress tensor normal to the base *b* of the interface element and, therefore, is able to describe the crack process in mode one. Thus, the damage criterion is written as:

$$\theta = \bar{\sigma}_{nn} - s(r) \leq 0 \tag{13}$$

where $\bar{\sigma}_{nn}$ is the component of the stress tensor normal to the base *b* of the interface element and *s* and *r* are the stress and strain-like internal variables, respectively. Manzoli *et al.* (2014), Maedo *et al.* (2014) and Sánchez *et al.* (2014) describe in detail the tensile damage model used in this work.

6. NUMERICAL EXAMPLES

The mesh fragmentation technique consists of introducing interface elements throughout the mesh or just the region of interest, thereby aiming at reduction in processing time and computational effort.

For the simulated cases, all the elements are linear triangular elements. The bulk elements have linear elastic behavior and interface elements are represented by damage model.

To insert interface elements consists of decreasing the bulk elements and accommodate a pair of interface elements in the adjacent space, as shown in Fig. 2.

In all cases simulated in this work was considered a constant fluid injection rate $q = 1.10^{-7}\frac{m^3}{s}$, reference density $\rho_0 = 1002,6\frac{kg}{m^3}$, reference pressure $0,1$MPa and fluid's isothermal compressibility factor $\beta = 4,5.10^{-4}\text{MPa}^{-1}$.

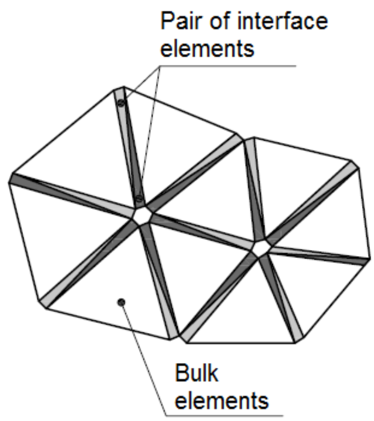

Figure 2. Mesh fragmentation technique (adapted from Maedo *et al.* (2014)).

6.1 Variation of Permeability

In this first study it was simulated an area of 10×10m with half of a well of $0,6$m diameter located to the left side of center. The geometry and the boundary conditions are illustrated in Fig. 3. Symmetry conditions were imposed across the left side.

Figure 4 shows the mesh used. Only the central horizontal strip has been fragmented, because is expected that the fracture is developed in this region, and reduce the processing time.

Four cases were simulated considering a "*extended Leak-Off Test*" (Hamidi and Mortazavi, 2014) with different permeabilities, aiming to determine their influence about the behavior of fracture. Table 1 shows the mechanical and hydraulic properties used in elements that represent the rock. Table 2 shows properties of the interface elements used. Only interface elements can be degraded, thus the fracture occurs where they are located, i.e., skirting the bulk elements.

Table 1. Properties of regular elements

Mechanical Properties		Hydraulic Properties	
Young's modulus	$E = 32$GPa	Intrinsic permeability	$k =$ 1.10^{-16}m^2 1.10^{-17}m^2 1.10^{-18}m^2 1.10^{-19}m^2
Poisson's ratio	$\nu = 0.2$	Porosity	$\phi = 0.1$

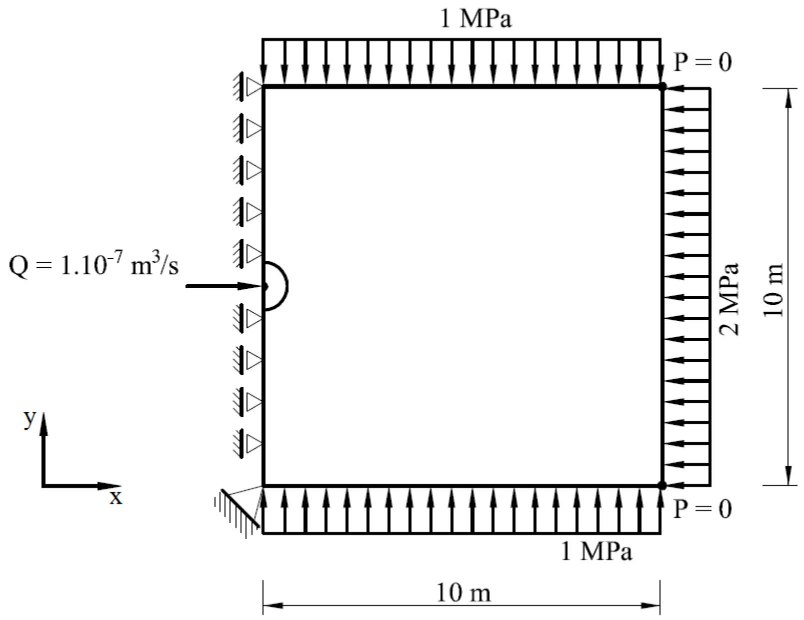

Figure 3. Geometry and mechanical and hydraulic boundary conditions.

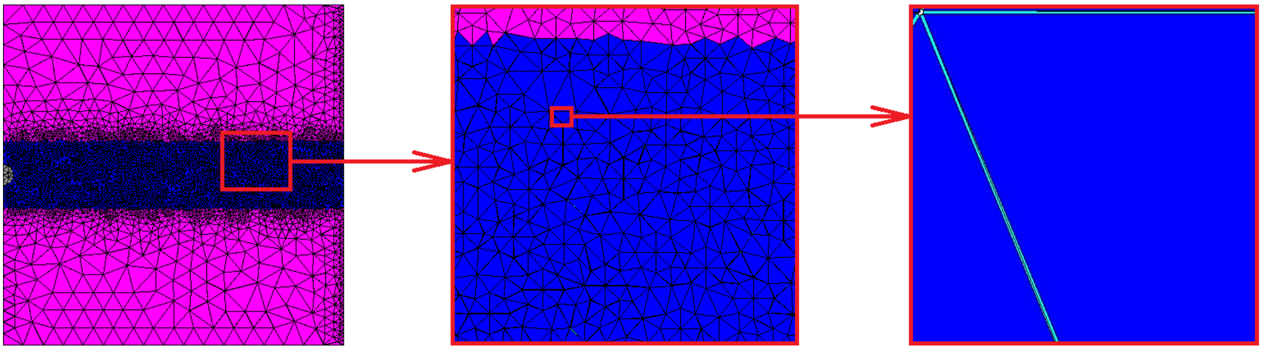

Figure 4. Finite element mesh used. The central strip of blue color indicates that only this region was fragmented.

Table 2. Properties of interface elements

Mechanical Properties		Hydraulic Properties	
Young's modulus	$E = 32\text{GPa}$	Intrinsic permeability	$k =$ 1.10^{-16}m^2 1.10^{-17}m^2 1.10^{-18}m^2 1.10^{-19}m^2
Poisson's ratio	$\nu = 0.0$	Porosity	$\phi = 0.1$
Tensile strength	$f_t = 2.8\text{MPa}$		
Fracture energy	$G_t = 98\text{N/m}$		

Figure 5 shows the pressure behavior in the well over time. The first peak of each curve corresponds to breakdown pressure. Yew (1997) presents a equation to determine the breakdown pressure, which results in $3,8$MPa using parameters in this work. Considering that the three first peaks (Fig. 5) occurs approximately in $4,1$MPa, the percentage error is equal 8%. It is noticed also that there is a minimum permeability to occurs a hydraulic fracture.

Figure 6 shows the behavior of the rock with $k = 1.10^{-18}\text{m}^2$ over time. Note that the pressure gradient is uniform and radial while there is no fracture, showing that the fluid is penetrating the rock. After initiation of the fracture, the pressure around the well decreases and appears a pressure gradient in the walls of the fracture. Guo *et al.* (1993) show that the fracture propagates perpendicular to the least principal stress.

Figure 7 shows the behavior of the rock with $k = 1.10^{-16}\text{m}^2$ over time. Note that when there is much loss of liquid through the rock, the pressure is not enough to fracture it.

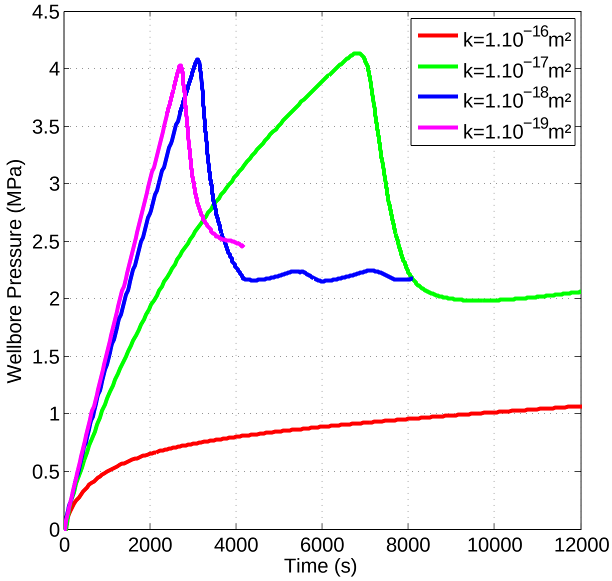

Figure 5. Pressure behavior in well to different permeabilities. In the case of higher permeability (1.10^{-16}m^2) does not fracture occurred, since there was plenty of liquid penetration into the rock.

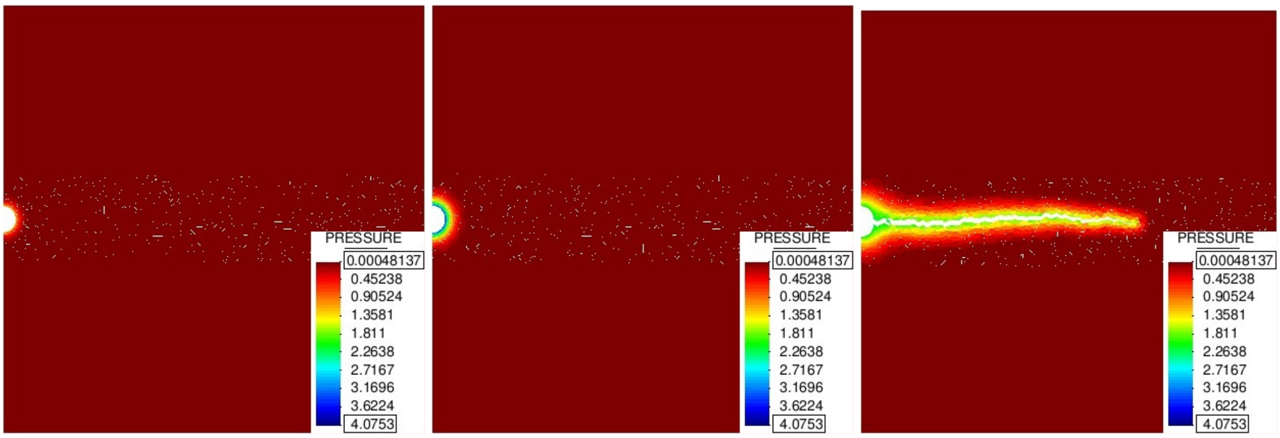

(a) $t = 1081s$ (b) $t = 3025s$ (c) $t = 5050s$

Figure 6. Pressure gradient considering $k = 1.10^{-18}\text{m}^2$.

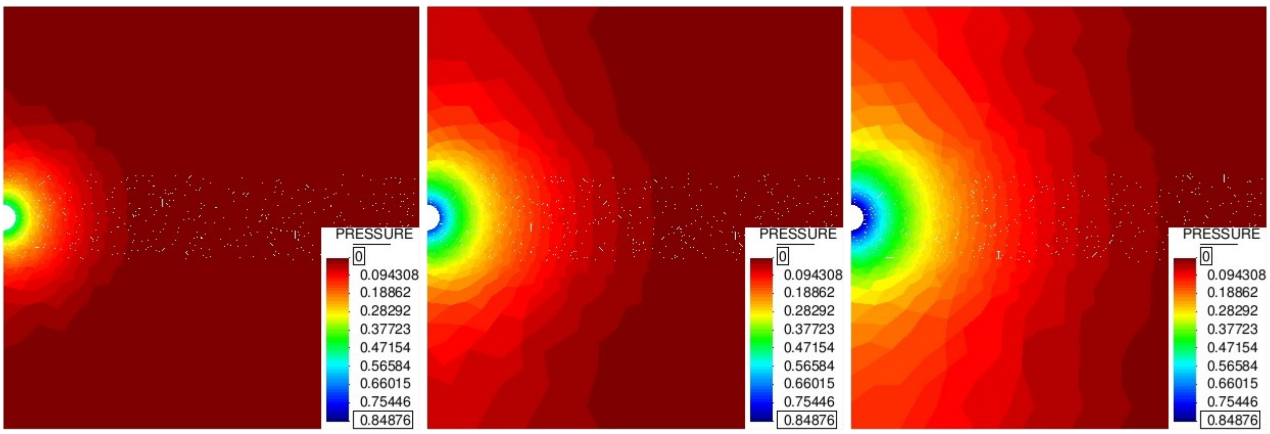

(a) $t = 1081s$ (b) $t = 3025s$ (c) $t = 5050s$

Figure 7. Pressure gradient considering $k = 1.10^{-16}\text{m}^2$.

6.2 Thickness Variation of Interface Elements

This case considers a problem in the same condition shown in Fig. 3. The characteristics of the bulk elements are shown in Table 1 and the characteristics of the interface elements are shown in Table 2, but both consider only the intrinsic permeability $k = 1.10^{-18}\text{m}^2$.

The study was based on the verification of the influence of the height of the interface elements on the formation of the fracture. Thus, first, a continuous case was simulated, which has not fragmented and verified the variation of the wellbore pressure over time. After four fragmented meshes were considered and the height of interface elements was different for each mesh.

Figure 8 shows the structural response of non-fragmented mesh and the four fragmented meshes. Note that the smaller the height *h* of the interface elements, the structural response approaches the continuous medium. The breakdown pressure values is practically equal to different heights, being close to 4MPa.

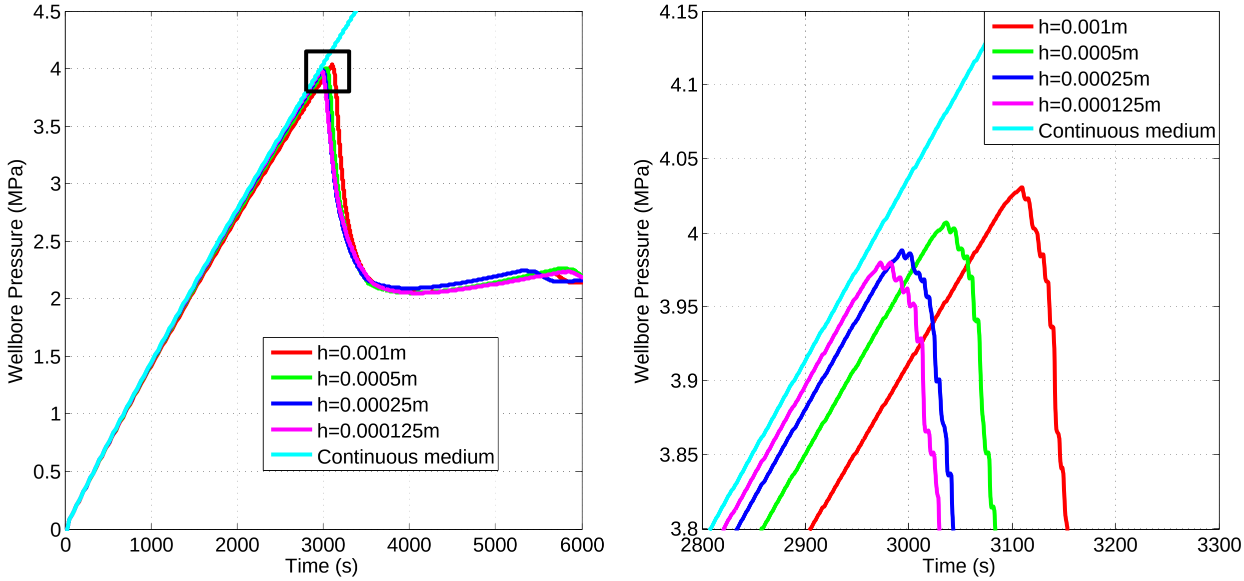

Figure 8. Different thicknesses of interface elements. Note that the rupture pressure is very similar for all four cases.

7. CONCLUDING REMARKS

The fragmentation technique consists of inserting solid finite elements with a high aspect ratio between the bulk elements of the mesh. This technique proved to be effective in predicting fractures generated hydraulically, which adequately represents the initiation and propagation of fractures.

The interface elements were able to capture the hydraulic and mechanical behavior of the hydraulic fracturing phenomenon, showing that highly permeable rocks do not fracture and and that different heights has no significant influence on the breakdown pressure.

The structural responses obtained showed that this technique is consistent with analytical results. It was possible to detect that when the fluid pressure reaches the breakdown pressure, the fracture occurs. Furthermore, the propagation direction of the fracture showed to be perpendicular to the smallest principal stress.

8. ACKNOWLEDGEMENTS

The authors wish to thank the financial support provided by CAPES (Coordenação de Aperfeiçoamento de Pessoal de Nível Superior), CNPq (Conselho Nacional de Desenvolvimento Científico e Tecnológico) and FAPESP (Fundação de Amparo à Pesquisa do Estado de São Paulo).

9. REFERENCES

Guo, F., Morgenstern, N. and Scott, J., 1993. "An experimental investigation into hydraulic fracture propagation-part 2. single well tests". In *International journal of rock mechanics and mining sciences & geomechanics abstracts*. Elsevier, Vol. 30, pp. 189–202.

Hamidi, F. and Mortazavi, A., 2014. "A new three dimensional approach to numerically model hydraulic fracturing process". *Journal of Petroleum Science and Engineering*.

Huitt, J., 1956. “Fluid flow in simulated fractures”. *AIChE Journal*, Vol. 2, No. 2, pp. 259–264.

Li, L., Tang, C., Li, G., Wang, S., Liang, Z. and Zhang, Y., 2012. “Numerical simulation of 3d hydraulic fracturing based on an improved flow-stress-damage model and a parallel fem technique”. *Rock mechanics and rock engineering*, Vol. 45, No. 5, pp. 801–818.

Maedo, M., Manzoli, O., Rodrigues, E. and Cleto, P., 2014. “Simulação computacional por elementos finitos de propagação de múltiplas fissuras em sólidos usando técnica de fragmentação da malha”. *Anais do VIII Congresso Nacional de Engenharia Mecânica*.

Manzoli, O., Gamino, A., Rodrigues, E. and Claro, G., 2012. “Modeling of interfaces in two-dimensional problems using solid finite elements with high aspect ratio”. *Computers & Structures*, Vol. 94, pp. 70–82.

Manzoli, O., Maedo, M., Rodrigues, E. and Bittencourt, T., 2014. “Modeling of multiple cracks in reinforced concrete members using solid finite elements with high aspect ratio”. *Computational Modelling of Concrete Structures*, p. 383.

Marin, I.S.P., 2011. *Aperfeiçoamento do Método de Elementos Analíticos para Simulação de Escoamento em Rochas Porosas Fraturadas*. Ph.D. thesis, Escola de Engenharia de São Carlos.

Naveira, V.P., 2008. *Incorporação dos Efeitos Geomecânicos de Compactação e Subsidência na Simulação de Reservatórios de Petróleo*. Master’s thesis, Universidade Federal do Rio de Janeiro.

Oliver, J., 2000. “On the discrete constitutive models induced by strong discontinuity kinematics and continuum constitutive equations”. *International Journal of Solids and Structures*, Vol. 37, No. 48, pp. 7207–7229.

Oliver, J., Cervera, M. and Manzoli, O., 1999. “Strong discontinuities and continuum plasticity models: the strong discontinuity approach”. *International journal of plasticity*, Vol. 15, No. 3, pp. 319–351.

Oliver, J. and Huespe, A., 2004. “Continuum approach to material failure in strong discontinuity settings”. *Computer Methods in Applied Mechanics and Engineering*, Vol. 193, No. 30, pp. 3195–3220.

Rouainia, M., Lewis, H., Pearce, C., Bicanic, N., Couples, G. and Reynolds, M., 2006. “Hydro-geomechanical modelling of seal behaviour in overpressured basins using discontinuous deformation analysis”. *Engineering geology*, Vol. 82, No. 4, pp. 222–233.

Sánchez, M., Manzoli, O.L. and Guimarães, L.J., 2014. “Modeling 3-d desiccation soil crack networks using a mesh fragmentation technique”. *Computers and Geotechnics*, Vol. 62, pp. 27–39.

Snow, D.T., 1965. *A parallel plate model of fractured permeable media*. Ph.D. thesis, University of California.

Witherspoon, P., Wang, J., Iwai, K. and Gale, J., 1980. “Validity of cubic law for fluid flow in a deformable rock fracture”. *Water resources research*, Vol. 16, No. 6, pp. 1016–1024.

Yaquetto, N.P.R., 2011. *Avaliação de Esquemas de Acoplamento na Simulação de Reservatórios de Petróleo*. Master’s thesis, Pontifícia Universidade Católica do Rio de Janeiro.

Yew, C.H., 1997. *Mechanics of hydraulic fracturing*. Gulf Professional Publishing.

10. RESPONSIBILITY NOTICE

The authors are the only responsible for the printed material included in this paper.